Physical and Numerical Models on Mechanically Stabilized Earth Walls Using Self-Fabricated Steel Reinforcement Grids Applied for Cohesive Soil in Vietnam

Truong-Linh Chau *, Thu-Ha Nguyen *, Van-Ngoc Pham *

Posted Date: 28 December 2023

doi: 10.20944/preprints202312.2208.v1

Keywords: MSE wall; self-fabricated steel reinforcement grids; tensile forces; lateral displacement of the wall facing; failure surface; full-scale model; numerical model

Article

Physical and Numerical Models on Mechanically Stabilized Earth Walls Using Self-Fabricated Steel Reinforcement Grids Applied for Cohesive Soil in Vietnam

Truong-Linh Chau [1,*], Thu-Ha Nguyen [2,*] and Van-Ngoc Pham [3,*]

[1] Faculty of Bridge and Road Engineering, The University of Danang - University of Science and Technology, 54 Nguyen Luong Bang St., Danang City 550000, Vietnam E-mail: ctlinh@dut.udn.vn; Orcid: 0000-0003-4519-2723

[2] Faculty of Bridge and Road Engineering, The University of Danang - University of Science and Technology, 54 Nguyen Luong Bang St., Danang City 550000, Vietnam E-mail: ntha@dut.udn.vn; Orcid: 0009-0001-6223-2005

[3] Faculty of Bridge and Road Engineering, The University of Danang - University of Science and Technology, 54 Nguyen Luong Bang St., Danang City 550000, Vietnam E-mail: pvngoc@dut.udn.vn, Orcid: 0000-0002-3853-57273

* Correspondence: V.N. Pham: pvngoc@dut.udn.vn; Tel.: +84 869 400 900; T.H. Nguyen: ntha@dut.udn.vn; Tel.: +84 905 470 047; T.L. Chau: ctlinh@dut.udn.vn; Tel.: +84 913 422 267.

Abstract: The study examines the behavior of the Mechanically Stabilized Earth (MSE) wall using available reinforcement materials in Danang, Vietnam. The MSE was reinforced by the self-fabricated galvanized steel grids using CB300V steel with 3 cm ribs. The backfill soil is a sandy clay soil from the local area with a low cohesion. A full-scale model with full instrumentation was installed to investigate the distribution of tensile forces along the reinforcement layers. The highest load that caused the wall to collapse due to internal instability (reinforcement rupture) was 302 kN/m^2, which is 15 times the design load of 20 kN/m^2. The failure surface within the reinforced soil had a parabolic sliding shape which is similar to the theoretical studies. At the failure load level, the maximum lateral displacement at the top of the wall facing was small (3.9 mm) which is significantly lower than the allowable displacements for the retaining wall. Furthermore, a numerical model using FLAC software was applied to simulate the performance of the MSE wall. The modeling results are in good agreement with the physical model. Thus, the self-fabricated galvanized steel grids could be confidentially used in combination with the local backfill soil for the MSE walls.

Keywords: MSE Wall; self-fabricated steel reinforcement grids; tensile forces; lateral displacement of the wall facing; failure surface; full-scale model; numerical model

1. Introduction

Mechanically Stabilized Earth (MSE) walls are one of the types of retaining walls constructed to maintain the stability of the soil in the bridge abutment or high embankment. This technique was used in France in the 1960s and has since been widely applied in construction in many countries all over the world [1,2]. The structure of the MSE walls includes the backfill material (e.g., natural soil, fly ash, sand, geofoam), the reinforcement (e.g., geogrid, geotextiles, steel strips, steel grids), and the wall facing elements (e.g., rigid concrete panel, metal sheets, wood panels). The MSE retaining walls could resist the earth pressure, the service loads, and seismic loads with high stability and with a construction cost approximately 25-50% lower than conventional concrete or steel walls [1,3].

The MSE walls' behavior is complicated. The MSE walls' performance is established by the interactions between the soil and the reinforcement, the soil and the facing elements [4]. The stability of the MSE walls depends on some factors, including the type and the size of reinforcement, the properties of the backfill material, the construction techniques, the type of facing elements, and others [3,5,6].

 doi:10.20944/preprints202312.2208.v1

The mechanical behavior of the MSE wall was investigated using physical models by several researchers, such as Murray and Farrar [7], Chang, et al. [2], Lee, et al. [8], Richards, et al. [9], and Ahmadi, et al. [10]. These studies found that the failure surface of the wall had a parabolic shape, passing through locations with the highest tensile forces within the reinforcement layers [2,7,8,10,11]. The failure surface of the wall aligned with the horizontal direction at an angle of $(45^0 + \varphi/2)$ at the toe of the wall [10]. Currently, according to the design rules and standards [12–14], the failure surface of the MSE wall closely resembles the failure surfaces observed in the studies [2,7,8,10,11].

Khan, et al. [4], Ahmadi and Bezuijen [5], Kibria, et al. [15], Roscoe and Twine [16], Jensen [17], and Weldu [18] conducted full-scale and physical models to examine the behavior of the MSE walls, including the maximum tensile forces in the reinforcement, the connection between the reinforcement and the wall, horizontal pressure, and vertical pressure on the backfill. The results showed that the length of reinforcement and the reinforcement strength are the two most influential factors on the lateral displacement of the wall [15,17,18]. In addition, the tensile forces and deformation of the reinforcement depend on the uniformity coefficient (C_u) of the backfill soil [18].

Khan, et al. [4], Ho and Rowe [19], Yu, et al. [20], Weerasekara [21], Sadat, et al. [22], Powrie, et al. [23], and Zhang, et al. [24] investigated the stability of MSE walls through numerical models using FLAC software. The research results showed that the L/H ratio (where H is the wall's height and L is the length of the reinforcement) significantly influences the internal stability of the wall, and the optimal length of the reinforcement was suggested as L = 0.7H [19].

Furthermore, the elastic modulus of the foundation layer and backfill material, the shear resistance of the backfill material, and the tensile strength of the reinforcement all affect the tensile forces within the reinforcement layers [20,21]. The failure surface of the wall is similar to the Rankine failure surface [24].

The mentioned studies analyzed the stress-strain relationship within MSE wall structures, including determining the failure surface of the wall, the ultimate tensile rupture limit, the maximum wall displacement, the optimal length of reinforcement, and the reasonable spacing for reinforcement placement within the wall for different wall heights, the backfill materials, and the specific reinforcement materials. The primary factors influencing internal stability and overall stability of MSE walls are the backfill material (whether it is cohesive or granular and its properties), the type of reinforcement (rigid or flexible, strength, size, shape, and arrangement within the reinforced soil mass), and the foundation layer below the wall system.

In Vietnam, reinforcement elements such as steel strips or polymeric strips usually were imported from foreign suppliers with some critical issues. According to a design report by the Transportation and Transport Infrastructure Design Consultancy Company [25], the use of imported reinforcement materials can be up to 20-30% more expensive compared to using self-fabricated steel grid as reinforcement for the MSE walls [3]. Thus, it is beneficial to investigate the applicability of the self-fabricated steel reinforcement grids (e.g., CB300V steel with a diameter of 10 mm) as the reinforcement for MSE walls.

In addition, the backfill materials are suggested to meet the criteria of grain size distribution, low plasticity, and low fine content [26]. It is a fact that most natural backfill materials in the Central Coast of Vietnam are cohesive soil [3,27]. Hence, it is necessary to investigate the performance of the MSE wall (the stability of the MSE wall structure and the durability of the reinforcement) utilizing locally available backfill materials.

Moreover, in Vietnam, there has been very limited research on the stability of the MSE wall structure with the local reinforcements. Therefore, this study was conducted to investigate the performance of the instrumented MSE retaining wall. The research aims to observe the mechanical behavior of the MSE wall including the maximum tensile force and the load distribution in the reinforcement bars, the wall facing displacement, and the stability of the wall. To evaluate the global and compound (internal and external stability of the MSE walls), a full-scale model and a numerical model were applied in this study.

Preprints (www.preprints.org) | NOT PEER-REVIEWED | Posted: 28 December 2023 doi:10.20944/preprints202312.2208.v1

2. Full-scale experimental model

2.1. Model Design

The properties of the backfill material, the steel reinforcement, and the structural dimensions were chosen following the design rules and standards: Berg, et al. [1], BSI [13], AFNOR [12], and TCVN [14]. According to the AFNOR NF P94-270:2020 standard [12], the design load was 20 kN/m^2, and the experimental load was applied until the MSE wall to be collapsed, which includes reinforcement rupture.

The full-scale MSE wall was designed using the self-fabricated ribbed steel grids as the reinforcement. The dimensions of the MSE wall are shown in Figure 1. Within the scope of this study, the MSE wall was built on the rigid foundation which is assumed that the settlement is zero. Additionally, three lateral faces of the wall were fixed to restrict the expansion of the soil mass.

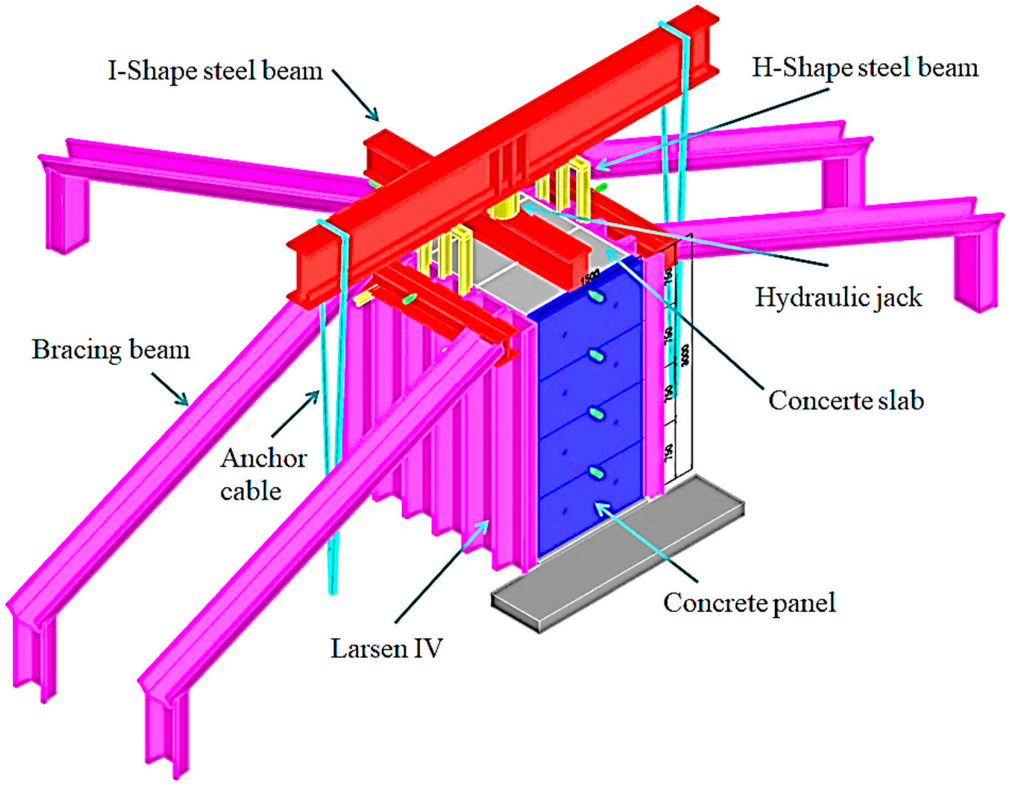

Figure 1. The test layout of the full-scale MSE model.

Wall facing panels

The wall facing was the rigid wall type, consisting of four precast Reinforced Concrete with Steel (RCWS) panels with concrete's strength of B22.5. The concrete facing panels with the dimensions of 1.5 x 0.75 x 0.14 m were used. The total height of the wall was 3 meters.

Backfill Material

Currently, most types of locally available backfill material in Danang City - Vietnam, are cohesive soil and they do not meet the requirements of mechanical, physical, and chemical properties to be reinforced backfill materials according to the standards [26,28].

In Danang City, the hillside soil from the Hoa Ninh area is the most suitable source of backfill material based on current standards [3]. Table 1 shows the mechanical, physical, and chemical properties of the local backfill material. The soil is sandy clay soil according to the standards AASHTO [26], AFNOR [12], and TCVN [14]. The particle size distribution and results of the standard proctor compaction test are shown in Figure 2. The grain sizes D60, D30, and D10 are 0.09, 0.65, and

Preprints (www.preprints.org) | NOT PEER-REVIEWED | Posted: 28 December 2023 doi:10.20944/preprints202312.2208.v1

4.1 mm respectively. The uniformity coefficient C_u was determined to be 45.6. The friction angle and the unit cohesion were 34.3^0 and 5.1 kN/m^2, respectively. The maximum dry density was 18.16 kN/m^3 when the optimum moisture content was 12.5%. The properties of the selected backfill material meet the requirements of the reinforced soil according to the standards AFNOR [12], AASHTO [26] and TCVN [14] for MSE wall construction.

However, the cohesion of 5.1 kN/m^2 in the backfill soil could affect the interaction between the steel reinforcement and the reinforced soil. In addition, this soil contains a remarkable amount of sulfate ion (SO_4^{-2} = 0.497 mg/g); thus it could affect the long-term durability of the reinforcement due to corrosion. Therefore, to efficiently utilize the available local backfill material, the reinforcement used in the wall was galvanized to prevent corrosion, and the soil-reinforcement interaction was enhance by arranging steel ribs on the reinforcement mesh.

The backfill soil was compacted using a light Tamping rammer (Niki NK55 from China) to ensure the soil had the same density. Each soil layer of 0.12 m height was compacted until achieving a relative density of 95% of the maximum dry density.

Table 1. Properties of the local backfill soil.

Parameter	Unit	Value
Saturated density, γ	kN/m^3	2.070
Dry density, γ_k	kM/m^3	1.816
Friction angle, φ_{soil}	degrees	34.3
Cohesion, c_{soil}	Pa	5100
Plasticity Index IP	-	8.55
Uniformity coefficient C_u	-	45.6
pH	-	5.9
Ion Cl^-	(mg/g)	0.094
Ion SO_4^{2-}	(mg/g)	0.497

Reinforcement

In this study, the self-fabricated galvanized steel grid (GSG) - CB300V steel with a diameter of 10 mm provided by the Viet Nhat Steel Joint Stock Company was used. The CB300V steel type has been widely used in Vietnam, and the Φ10 mm steel reinforcement meets the requirements for mechanical, physical, and chemical properties, as well as the design strength when used as the reinforcement in the MSE walls. The steel grid has 3 cm high ribs at the interaction of the longitudinal and transverse directions to increase the backfill soil-reinforcement interactions.

The tensile strength of the steel reinforcement (yield strength) – F_0 was 49,000 N. However, considering the effect of the backfill soil, the service life of the wall, the corrosion due to sulfate ions, and the metal loss during the 100-year design life of the MSE wall were included. Regarding the service life of the wall, Haiun, et al. [29] recommend that the MSE structure needs to be monitored and repaired when the values of remaining tensile strength within the reinforcement are equal to 65%F_0, with F_0 being the initial tensile strength of the reinforcement. Thus, in this study, at the initial stage, the tensile strength of the reinforcement was 31,850 N, as illustrated in Table 2.

Preprints (www.preprints.org) | NOT PEER-REVIEWED | Posted: 28 December 2023 doi:10.20944/preprints202312.2208.v1

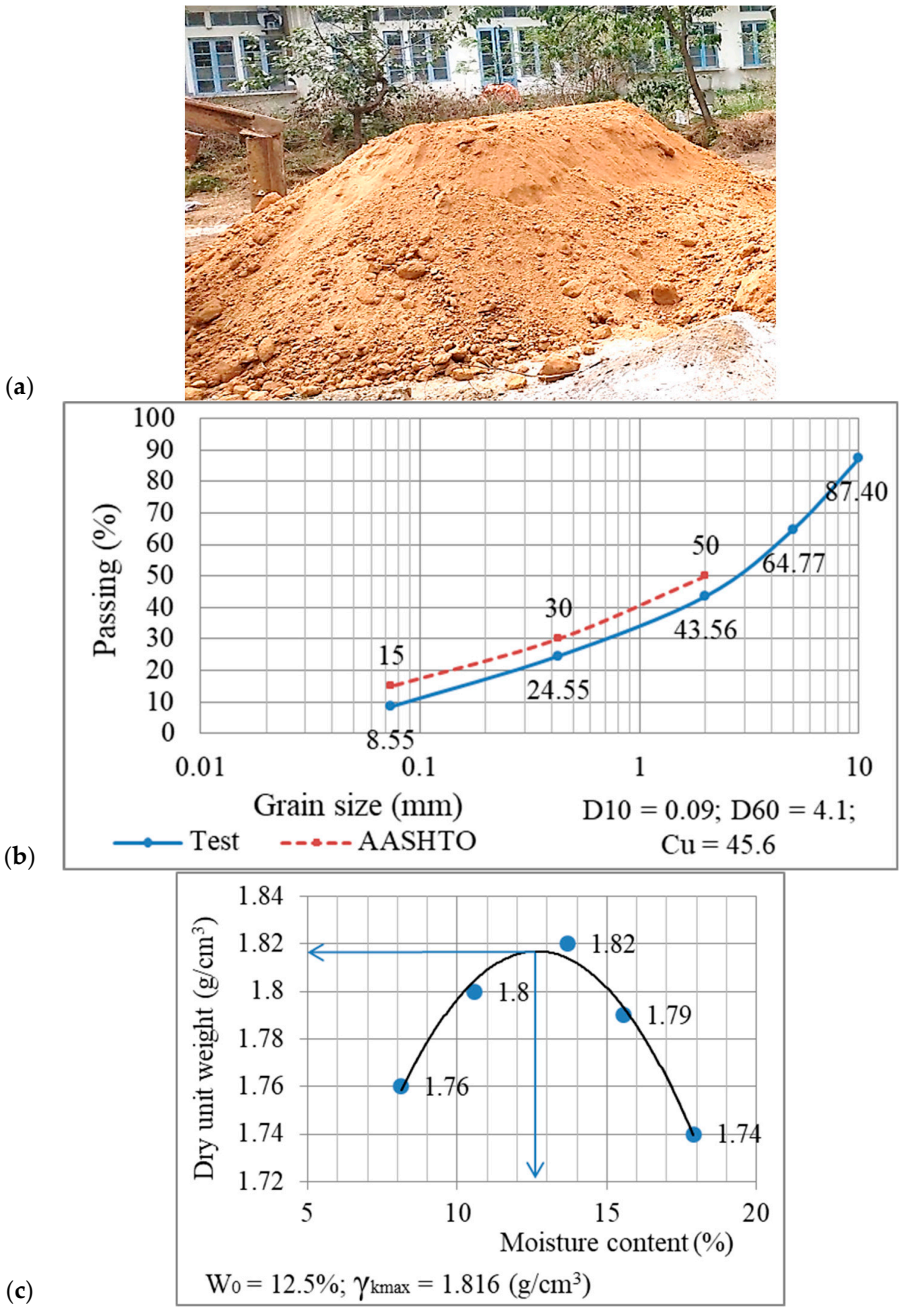

Figure 2. Properties of the backfill material.a. Local backfill soil; b. Grain size distribution of the backfill soil; c. Protor compaction results.

To consider the reduction in the tensile strength of the reinforcement, Haiun, et al. [29] performed drilling on the reinforcement bars to reduce their cross-sectional area. Furthermore, this method is also recommended in the design rules and calculation process for MSE walls in AFNOR NF P94-270:2020 [12]. Therefore, this study also carried out drilling to reduce the cross-sectional area of the reinforcement (as shown in Figure 3) with a proportional loss of tensile strength (ΔF) equal to 35%F_0, as indicated in Table 2.

Preprints (www.preprints.org) | NOT PEER-REVIEWED | Posted: 28 December 2023 doi:10.20944/preprints202312.2208.v1

Table 2. Reducing the cross-sectional area of the reinforcement bars.

Parameter	Unit	Value
Initial tensile strength of the steel reinforcement	N	49,000
Loss of tensile strength	N	17,150
Remaining tensile strength within the reinforcement	N	31,850
Drilling on the reinforcement bars to reduce their cross-sectional area	%	26.6
Drilling depth (Φ5)	mm	8.1

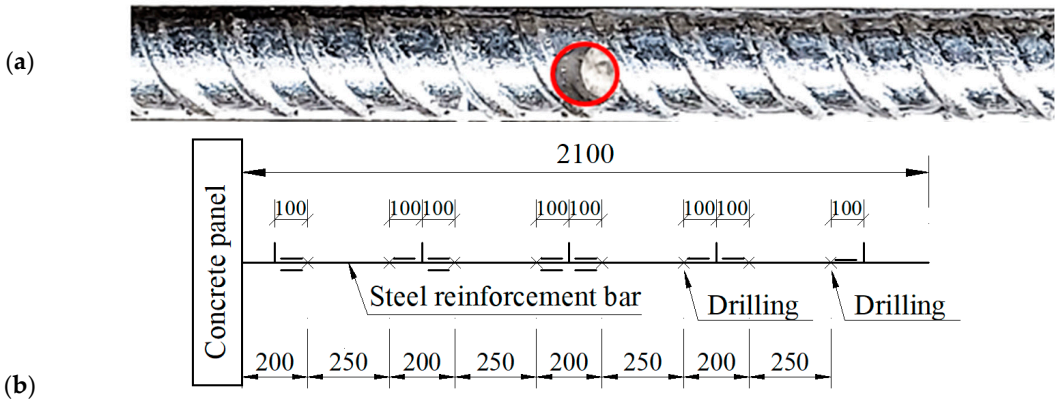

Figure 3. Drilling to reduce the cross-sectional area of the reinforcement bars. a. Drilling on the steel bar; b. Drilling postitions.

Furthermore, to enhance corrosion resistance for the reinforcement, the steel bars were galvanized by a zinc layer of 70 μm thickness. The length of the reinforcement bars was L = 2.1 m. The vertical spacing between the reinforcement layers was S_v = 0.75 m (4 reinforcement layers along the height of the wall H = 3 m). In each layer, 4 longitudinal steel reinforcement bars were installed with a space of 0.375 m. In addition, the horizontal spacing between the reinforcement bars (the transverse direction) was 0.45 m. The 3 cm high ribs were bonded at the reinforcement mesh to enhance soil-reinforcement interaction, as shown in Figure 4. The steel reinforcement grids were rigidly connected to the facing panels.

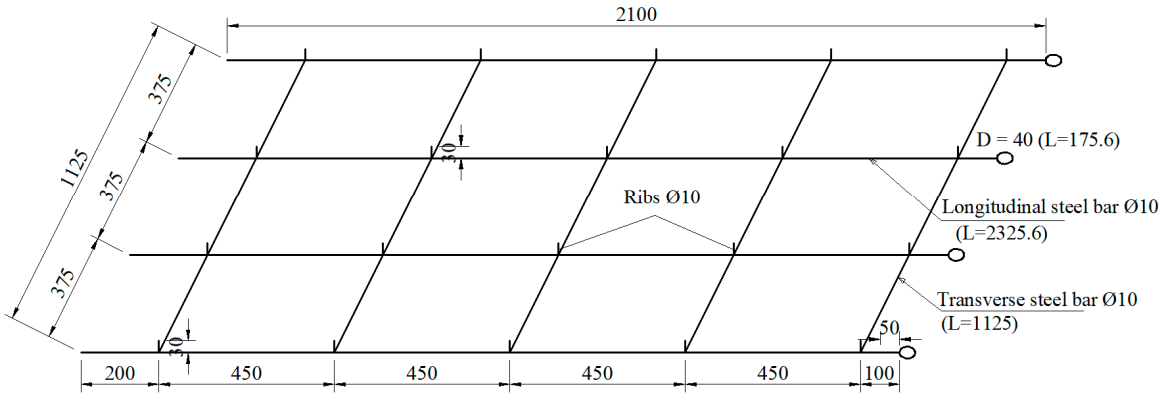

Figure 4. Design of the steel reinforcement grib.

The longitudinal steel reinforcement bars were installed at symmetrical locations. The initial test indicated that the deformation of all longitudinal steel reinforcement bars at the same layer is similar. Thus, in the following section, the behavior of one longitudinal steel reinforcement bar is presented.

Ground Foundation

 doi:10.20944/preprints202312.2208.v1

The MSE wall model was prepared and tested at the University of Danang – University of Science and Technology, Vietnam. The subgrade layer was compacted to achieve 95% of its relative density. On the top of this layer, a 20 cm thick layer of Reinforced Concrete with the dimension of 1.5 x 2.4 m was installed. This foundation was designed to ensure that the foundation remains stable without settlement during the construction and loading of the MSE wall.

Loading system

On the top of the retaining wall, 14 cm thick concrete plates were installed to transfer the load test from the loading system to the reinforced soil mass and the retaining wall. Three load plates with the dimensions of 1.5 x 0.75 x 0.14 m were used.

The load increment system included two anchor cables with the design load-bearing capacity of 1000 kN. In addition, the test loads were controlled using 200 T hydraulic jacks (TLP HHYG – 200150).

The boundary of the MSE wall model was fixed by steel sheet piles (Larsen IV) with dimensions of 400 x 170 x 15.5 mm. The steel sheet piles were driven to a depth of 2.8 m. The top of the wall was fixed by the bracing beams on three sides. This steel wall system is considered as a rigid boundary and prevents the displacements to the sides and the rear of the MSE wall.

2.2. Construction and instrumentation of the MSE wall

The MSE wall were constructed from the bottom up. The foundation soil was compated and the 20 cm thick concrete slab was installed. The steel sheet piles were driven to create the steel wall in three side of the model. The concrete facing panels, 15 cm thick backfill soil, and the steel reinforcement layers were installed in the correct order with full instrumentation. Finally, the loading system was constructed using concrete slab, steel frame, and anchor cables.

Figure 5 illustrates the layout of the model construction in the site before applying the test loads. The MSE wall was fully instrumented to observe the stress and strain distribution along the longitudinal reinforcement bars, the failure surface within the reinforced soil mass, the lateral displacement of the concrete wall facing, and the deformation of the boundary steel sheet wall.

The strain gauges (NIE-SG-CFA-120 - 5 cm long with 6 coils) manufactured in India were equipped for measuring deformations in the reinforcement and backfill material. The maximum deformation on the sensor is 2% (6 mm). These strain gauges were bonded in the steel reinforcement bars at the locations of 15, 50, 60, 95, 105, 140, 150, and 185 cm from the facing panel.

The lateral displacements of the steel sheet wall system, the anchor cables, and the wall panels were monitored by Linear Variable Differential Transformers (LVDTs) WYDC from Japan. with signal reading using the Data logger TDS 303 from Japan. LVDTs were installed at the top of concrete panels 2, 3, and 4 as shown in Figure 5a.

The vibrating wive Earth Pressure Cells (model 1910) manufactured by ACE Instrument in South Korea were installed to measure vertical and horizontal earth pressure at the top and the toe of the MSE wall. A Geokon 403 signal reader from the United States was used to read signals from the VW Earth Pressure Cell vibrating wire device during the testing process.

Temperature measurements within the wall using a metal thermometer, with a range of up to 100°C (used for calibrating readings from the resistive sensors and foundation surface pressure cell).

All instruments were calibrated before installation to ensure accurate measurements. In addition, the instruments were connected to the Data logger TDS 303 from Japan and a Geokon 403 signal reader from the United States for the data collection.

Preprints (www.preprints.org) | NOT PEER-REVIEWED | Posted: 28 December 2023 doi:10.20944/preprints202312.2208.v1

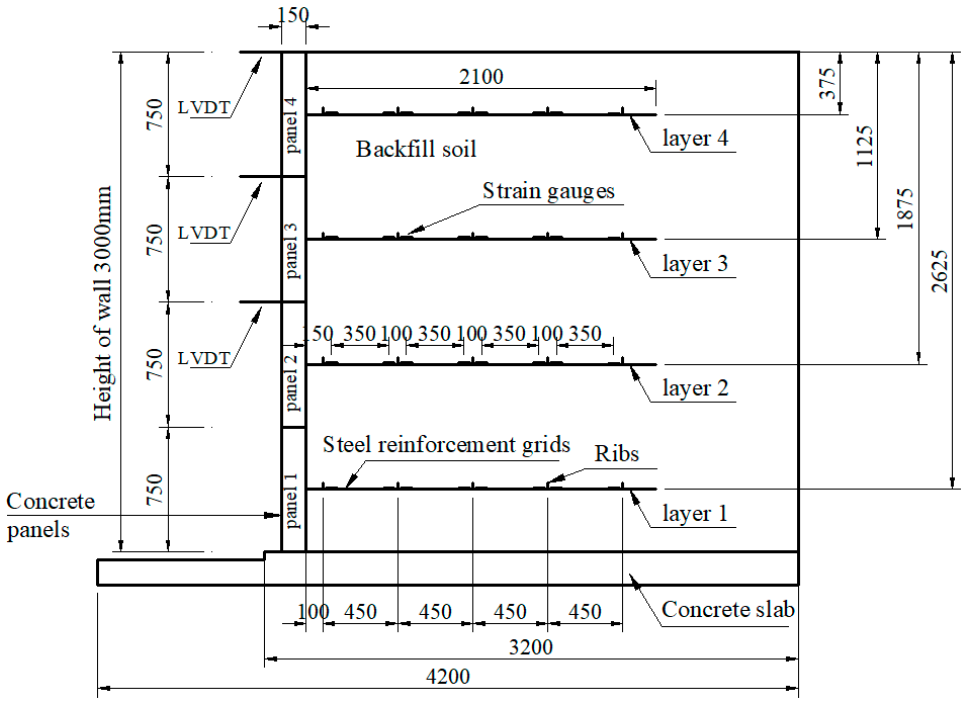

(a)

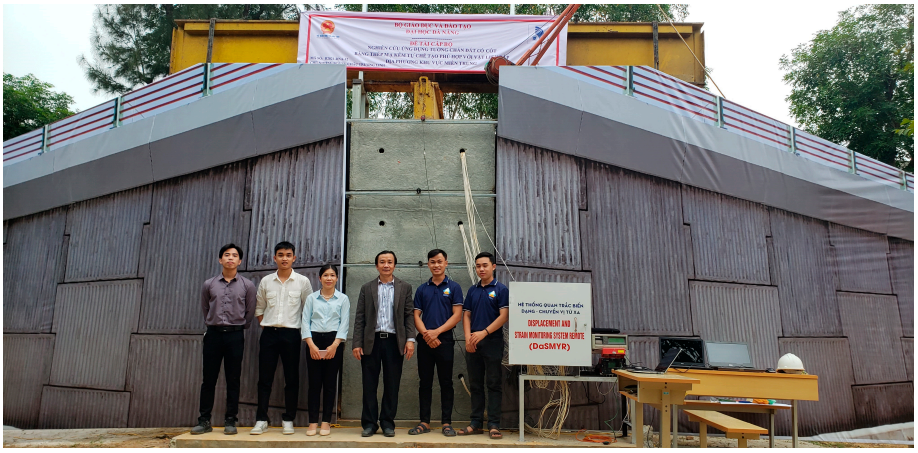

(b)

Figure 5. Full-scale MSE model with full instrumentation. a. MSE model with full instrumentation; b. Full-scale model after construction.

3. Numerical modelling

The finite difference program – FLAC [30] was used to simulate the performance of the MSE wall with the same dimensions as the full-scale model in section 2. The wall's height was 3 m and the length of the reinforcement bars was 2.1 m. The geometric details of the MSE wall in FLAC are shown in Figure 6.

Foundation soil was considered a rigid material with a high cohesion value (c = 55.1 MPa, φ = 51^0) and is 5 m deep below the wall system. The linear-elastic model using the Mohr-Coulomb failure criterion was used to simulate the backfill soil and the foundation soil. The backfill soil properties were modeled based on the experimental results as shown in Table 1. The concrete facing panels were simulated by beam elements and modeled as elastic materials with modulus E = 200 GPa. The strip elements in FLAC were used to model the steel reinforcement grid with a tensile strength of 31,850 N/m and tensile stiffness of 20,000 kN/m. Table 3 illustrates the properties of the concrete facing panel, backfill soil, and foundation materials.

Preprints (www.preprints.org) | NOT PEER-REVIEWED | Posted: 28 December 2023 doi:10.20944/preprints202312.2208.v1

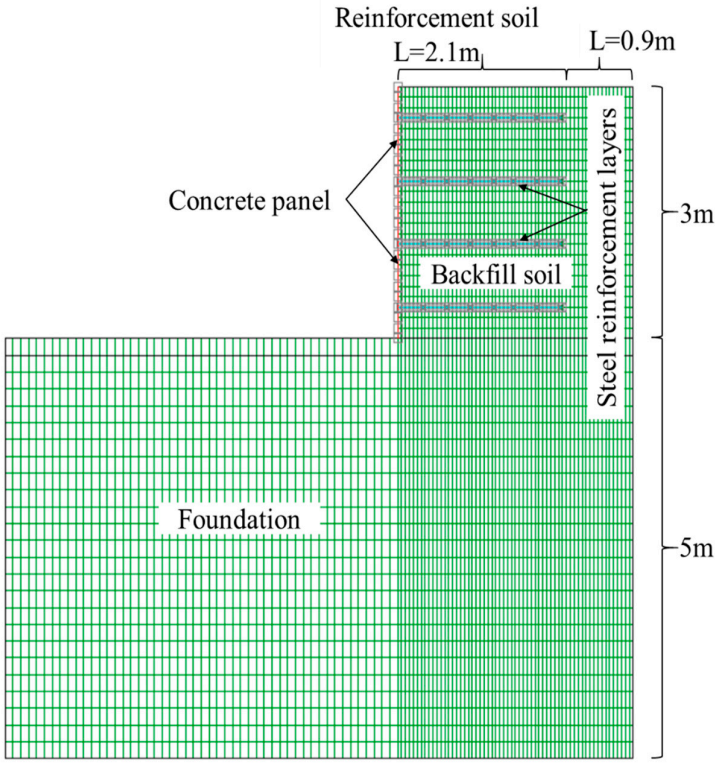

Figure 6. The MSE wall model in FLAC.

The interface between the backfill soil and concrete facing panel was modeled using the values suggested by Huang, et al. [31] and Huang, et al. [32]. In detail, the friction angle between the soil and concrete panel was 260; the interface normal stiffness was 2.4 MPa/m and shear stiffness was 2.4 MPa/m.

The apparent friction coefficients for the steel reinforcement and backfill interfaces were calculated based on the suggestion of current standards [8,12,13,33]:

– If $z > z_0 = 6$ m;

$$f^* = \tan\varphi \quad (1)$$

– If $z \le z_0 = 6$ m;

$$f^* = f_o^*(1-z/z_o)+(z/z_o)\tan\varphi \quad (2)$$

$$f_o^* = 1{,}2+\log_{10}(C_u); \quad (3)$$

where: f^* and f_o^* are the apparent friction coefficients for the steel reinforcement and backfill interfaces; C_u is the coefficient of uniformity of the backfill soil; z is the depth of the reinforcement layers from the top of the wall, $z_0 = 6$ m; φ is the friction angle of the backfill soil. Table 4 illustrates the properties of backfill-reinforcement interactions and facing panel–backfill interactions.

Table 3. The MSE model parameters in FLAC.

Parameter	Unit	Value
Concrete panel		
Width	m	0.75
Height	m	0.15
Length	m	1.5
Young's modulus	Pa	2.10^{11}
Compressive strength of concrete	MPa	35
Foundation soil		
Unit weight, γ_{Found}	kg/m^3	2700
Friction angle, φ_{Found}	degrees	51

Preprints (www.preprints.org) | NOT PEER-REVIEWED | Posted: 28 December 2023 doi:10.20944/preprints202312.2208.v1

Cohesion, c_{Found}	Pa	$5.51.10^7$
Bulk modulus	Pa	$4.39.10^{10}$
Shear modulus	Pa	$3.02.10^{10}$
Backfill soil		
Unit weight, γ_{soil}	kg/m^3	2070
Friction angle, φ_{soil}	degrees	34.3
Cohesion, c_{soil}	Pa	5100
Bulk modulus	Pa	$1.5.10^7$
Shear modulus	Pa	6.10^6
Steel reinforcements		
Length	m	2.1
Steel bar thickness	m	0.010
Calculation width	m	1.5
Number of longitutial bars per calculation width	strip	4
Young' modulus	Pa	2.10^{11}
Tensile strength	N/m	31850
Tensile failure strain	%	0.19
Shear stiffness	N/m^2	2.10^7

4. Results and discussion

4.1. Full-scale model results

MSE wall loading

The fully instrumented model was completed and loaded incrementally until the failure occurred in the MSE wall structure (fast displacement occurred or steel bar rupture). For each interval, the load increment was maintained for 30 minutes. The total dead loads from the steel beams and concrete slab were 12 kN/m^2. The design load on the model was 20 kN/m^2 [12]. The maximum load (when the steel reinforcement bars were ruptured) was 302 kN/m^2, approximately 15 times the normal traffic loading of 20 kN/m^2. The stress, strain, and displacement of the wall, the longitudinal reinforcement bars, and the reinforced soil mass were recorded at the load levels of 12, 20, 50, 75, 100, 150, 200, 250, 275, 300, and 302 kN/m^2.

Tensile Forces in the Reinforcement Bars

The tensile force F is calculated by Equation (4):

$$F = \frac{\Delta l.E.A}{L} \quad (4)$$

where: Δl is the measured deformation on the reinforcement bars; E is the elastic modulus of the reinforcement material, E = 210,000 MPa for the CB300V steel; A is the cross-sectional area of the reinforcement bars, with A = 78.5 mm^2; L is the length of the longitudinal reinforcement bars, with L = 2.1 m.

Table 4. Interface properties.

Parameter	Unit	Value
Backfill soil - Concrete panel		
Normal stiffness	Pa/m	$2.4.10^6$
Shear stiffness	Pa/m	$2.4.10^6$
Friction angle	degrees	26
Backfill soil- Steel reinforcements		
Shear stiffness	N/m^2	2.10^7
Cohension	N/m	1.10^5
Initial apparent friction coef:		
Layer 4		1.917

Preprints (www.preprints.org) | NOT PEER-REVIEWED | Posted: 28 December 2023 doi:10.20944/preprints202312.2208.v1

Layer 3	1.751
Layer 2	1.586
Layer 1	1.420

The distribution of tensile forces in each reinforcement layer is shown in Figure 7. It can be seen that when the test load increases from 12 kN/m² to 302 kN/m², the tensile forces in the reinforcement bars increase and create a sliding surface within the reinforced soil.

The maximum tensile force values were found at 95 cm further away from the facing panel in the reinforcement layers 3 and 4, and 60 cm (near the facing panel) in the reinforcement layers 2 and 1 (the reinforcement layers in deeper positions).

Figure 8 indicates that when the test load is lower than the design load (<20 kN/m²), the tensile forces in the deeper reinforcement layers are greater than the upper ones. However, when the test load is higher than 75 kN/m², the tensile forces in the reinforcement layers 3 and 4 are higher than the layers 1 and 2. It is a fact that at the low load level, the total load (including the earth pressure, dead loads, and surcharge load) increases with the depth of the wall. Thus, the deeper reinforcement layers absorb a greater load than the upper layers. Conversely, when the load test is high, the reinforcement layer 4 achieves the highest tensile forces, and this value decreases along the wall depth.

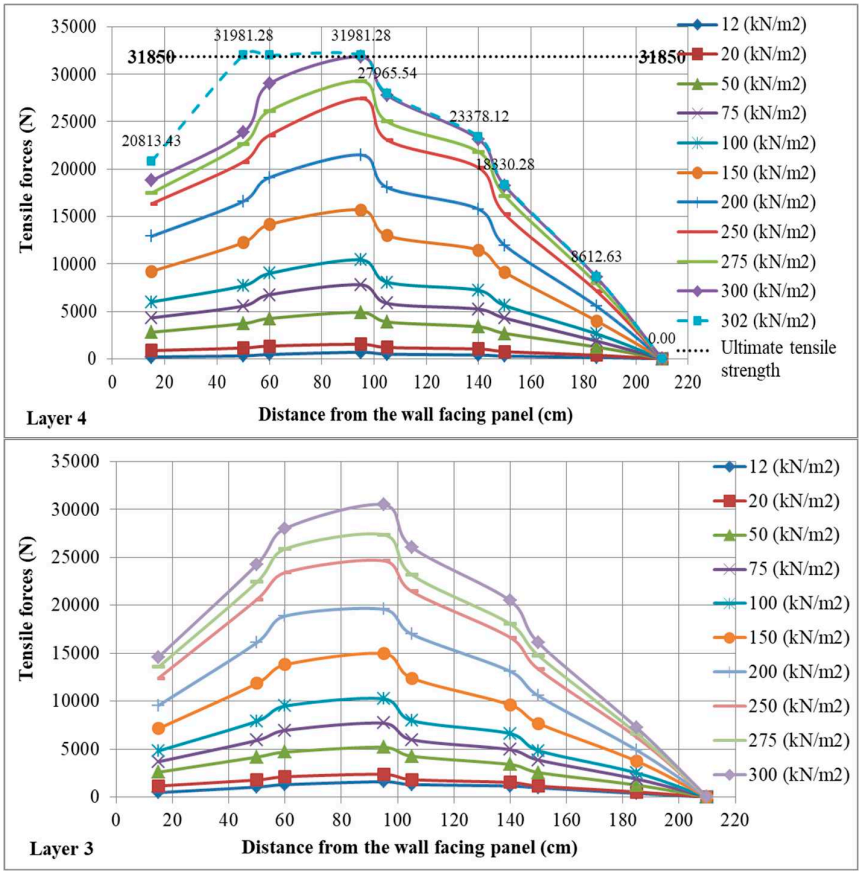

(a)

(b)

Preprints (www.preprints.org) | NOT PEER-REVIEWED | Posted: 28 December 2023 doi:10.20944/preprints202312.2208.v1

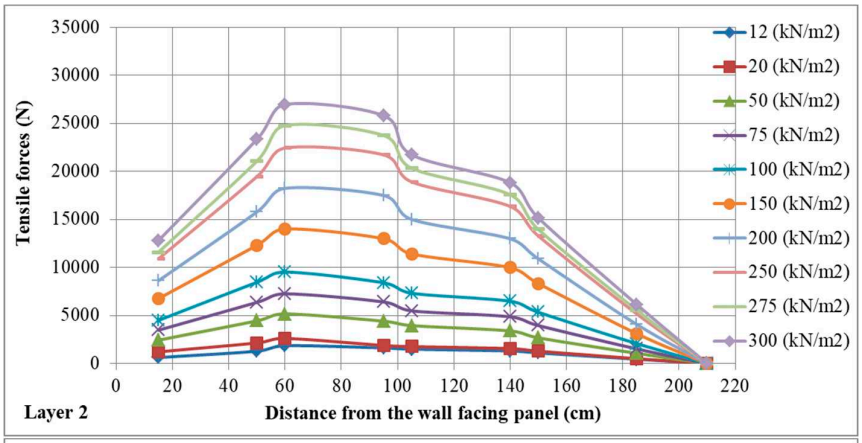

(c)

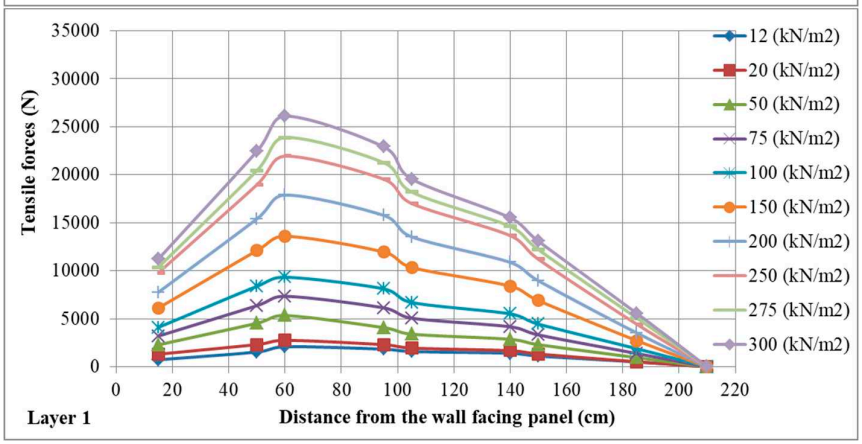

(d)

Figure 7. The tensile force distribution in the reinforcement layers at different test load levels. a. The 4th layer; b. The 3rd layer; c. The 2nd layer; d. The 1st layer.

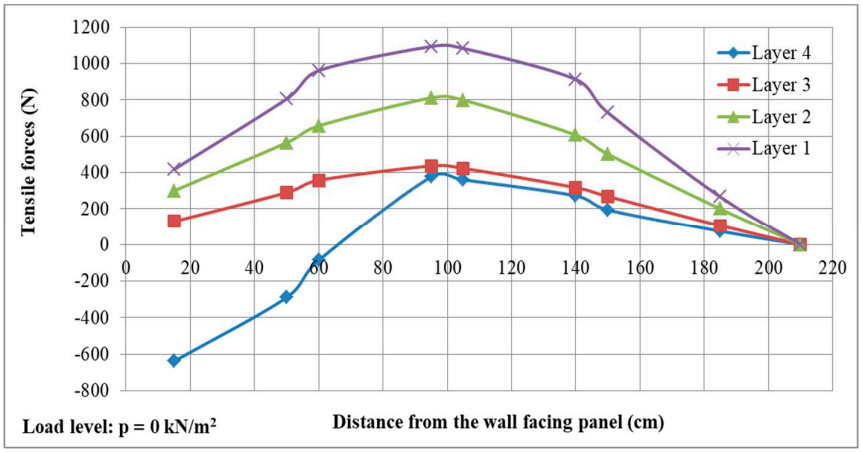

(a)

Preprints (www.preprints.org) | NOT PEER-REVIEWED | Posted: 28 December 2023 doi:10.20944/preprints202312.2208.v1

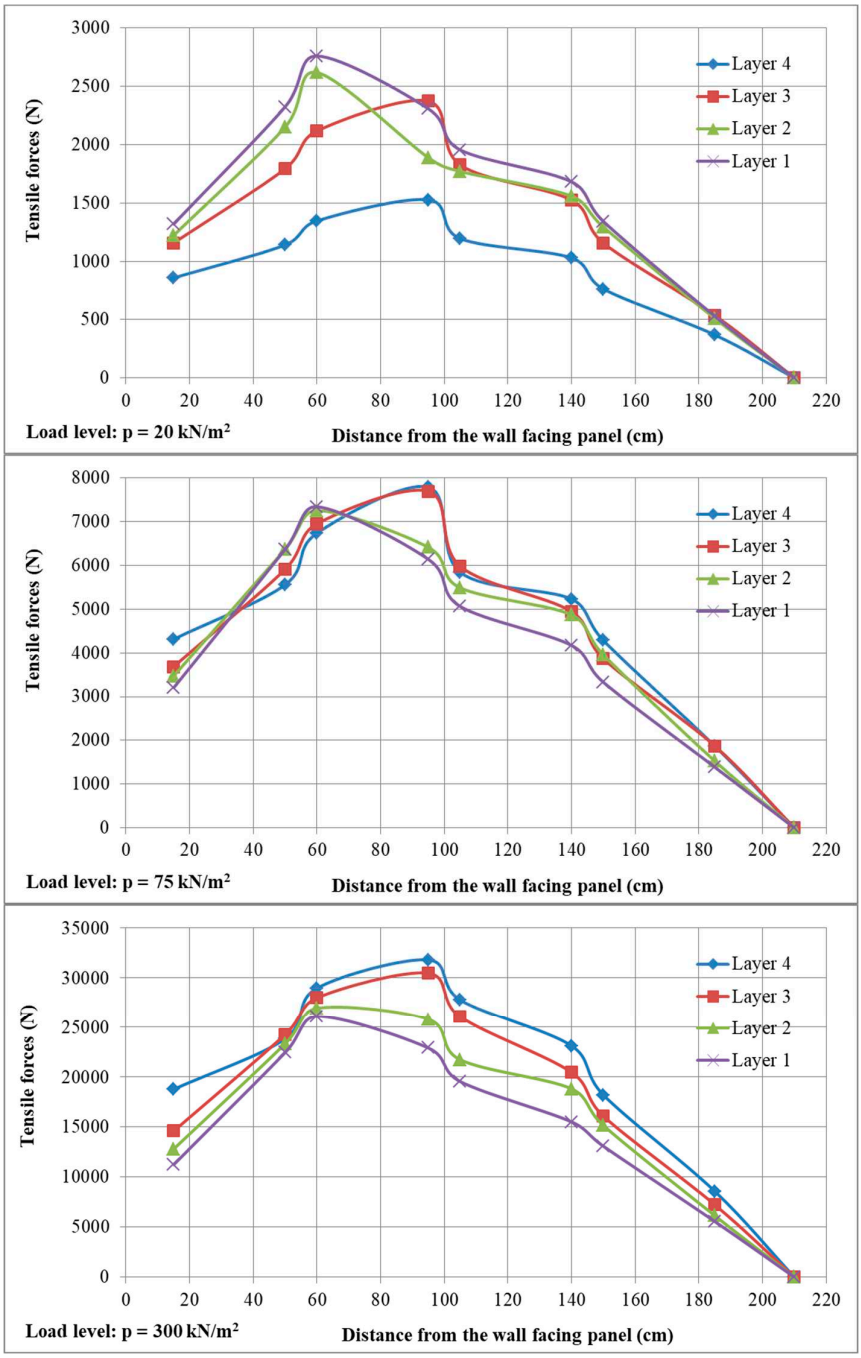

Figure 8. Tensile force distribution in different reinforcement layers. a. Load level of 0 kN/m²; b. Load level of 20 kN/m²; c. Load level of 75 kN/m²; d. Load level of 300 kN/m².

The distribution of the tensile force in the reinforcement layers from this study is similar to the reports of Schlosser [33], Wichter, et al. [34], Murray and Farrar [7], Chau, et al. [35], Chau and Nguyen [28], and the design procedures [12–14]. However, the steel ribs included in the reinforcement grids cause the step in the tensile force distribution curve in front of and behind the ribs. This result is reasonable and similar to the previous research results [36,37]. It indicates that the experimental results from this full-scale model are reliable and can be used in practice.

Preprints (www.preprints.org) | NOT PEER-REVIEWED | Posted: 28 December 2023 doi:10.20944/preprints202312.2208.v1

Failure load

In Figure 9, the maximum tensile force in the reinforcement bars was 31,823 N at the test load of 300 kN/m². When the load level was 302 kN/m², the maximum tensile force in the reinforcement layers was 31,881 N, which is higher than the ultimate tensile force of 31,850 N. Thus, at that moment, the failure occurred in the MSE wall. The longitudinal steel bars were suddenly ruptured at the drilling cross-sectional area where the tensile force reaches its maximum value in the reinforcement bars.

(a)

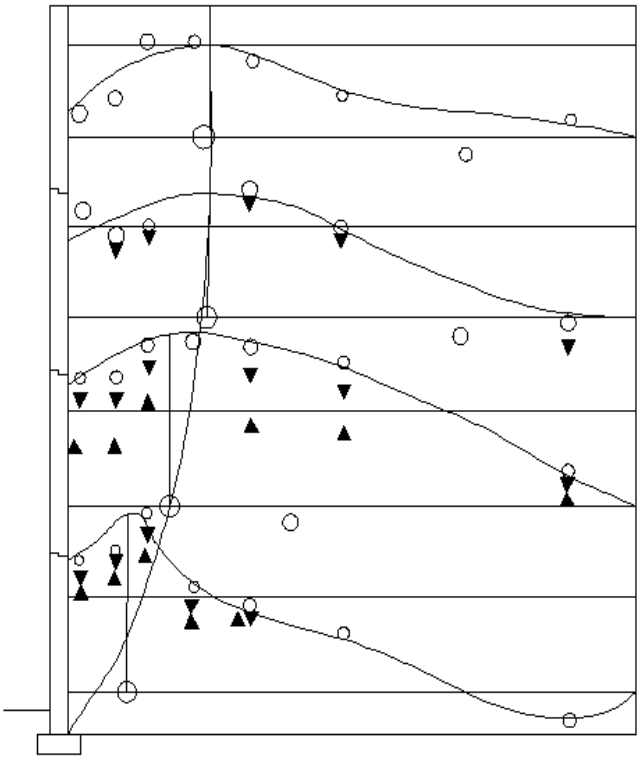

(b)

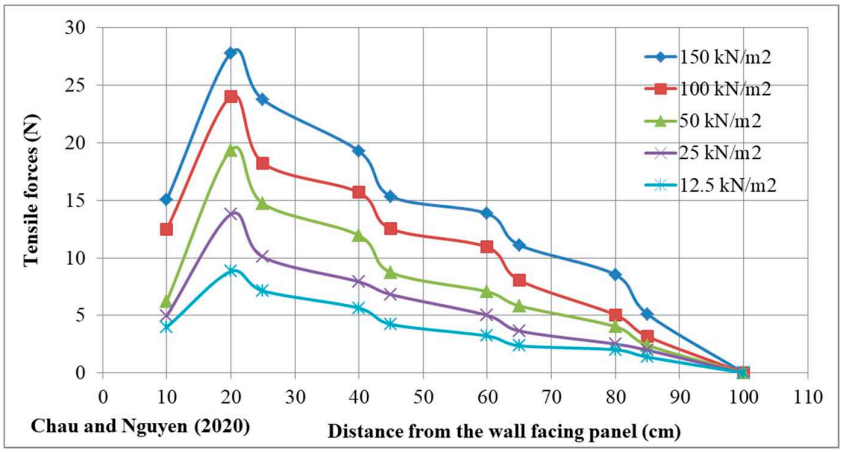

Preprints (www.preprints.org) | NOT PEER-REVIEWED | Posted: 28 December 2023 doi:10.20944/preprints202312.2208.v1

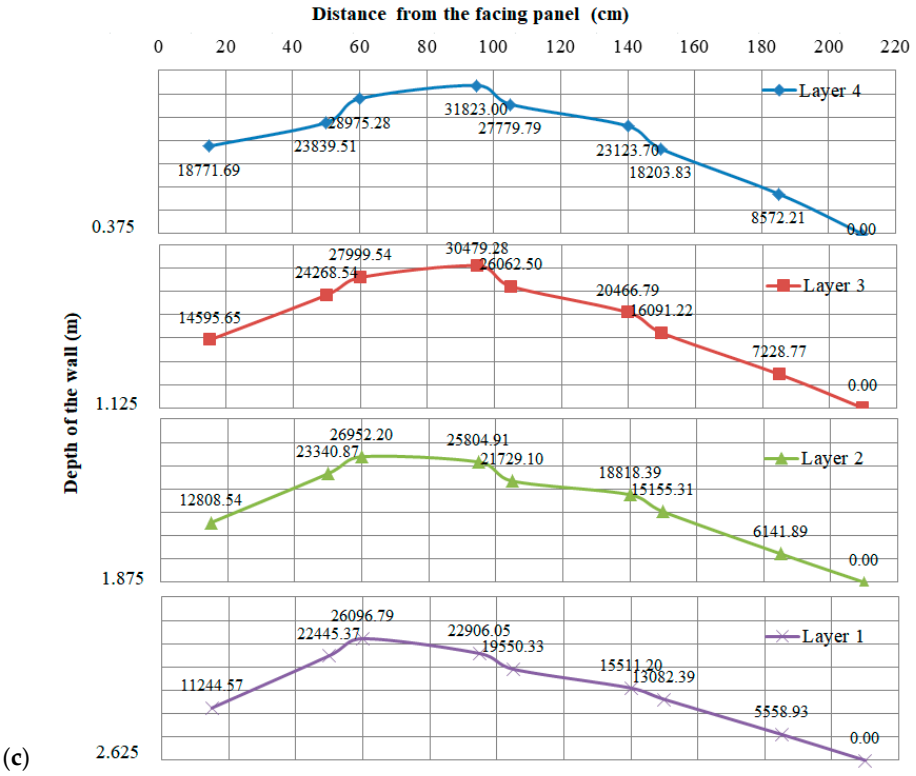

(c)

Figure 9. Tensile force distribution in different studies. a. Murray and Farrar [7]; b. Chau and Nguyen [28]; c. This study.

The failure load was determined to be 302 kN/m^2, which is 15 times the design load. In terms of load-bearing capacity, the MSE wall structure in the experimental model can resist a very high surcharge loads. However, in terms of long-term serviceability, the selected steel bars are appropriate with the structure durability during its service life of 100 years under the design load of 20 kN/m^2 [3].

At the failure load level of 302 kN/m^2, the failure surface in the reinforced soil could be determined by connecting the maximum tensile force points in each reinforcement layer. Figure 10 demonstrates that the failure surface in this study is similar to the Rankine theory [2]. In detail, in the first half of the wall, the failure surface starts from the top of the wall and further away from the wall face of approximately 0.3H. In deeper positions, the failure surface is closer to the wall facing and stops at the toe of the wall (wall base). This failure pattern is similar to the report of Chang, et al. [2], Lee, et al. [8], Murray and Farrar [7], Schlosser and Guilloux [36], and Murray [11].

Preprints (www.preprints.org) | NOT PEER-REVIEWED | Posted: 28 December 2023 doi:10.20944/preprints202312.2208.v1

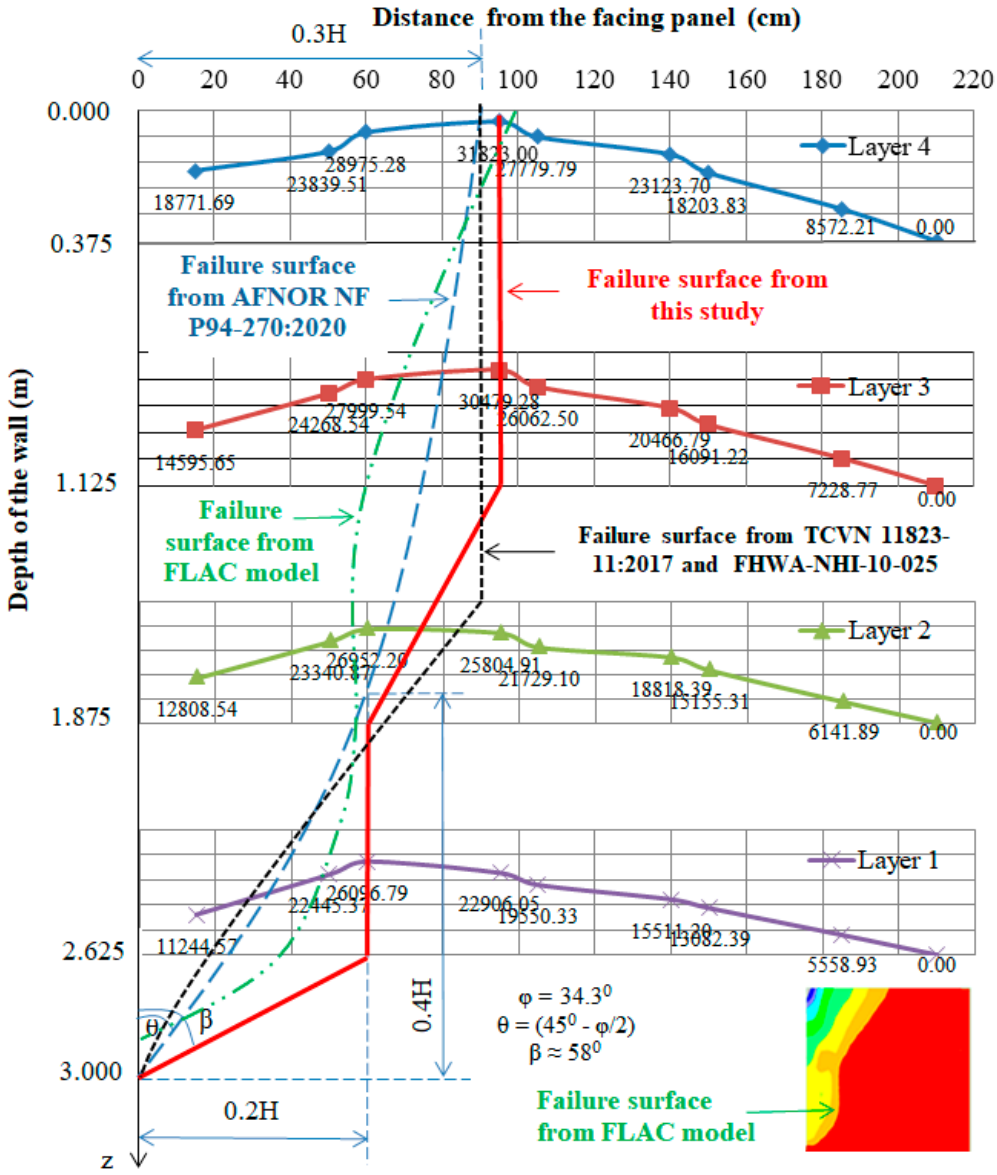

Figure 10. Failure surface in the reinforced soil mass.

Table 5 illustrates the length of the reinforcement bars in the failure zone L_a in this study and the values calculated from the standards AFNOR [12]. The L_a values in the reinforcement layers 4, 3, and 2 are close to the values estimated theoritically. The failure surface of the lowest layer is slightly different due to the strain gauge locations.

In summary, the failure surface in this full-scale MSE model using a cohesive backfill soil and self-fabricated steel reinforcement is in good agreement with other studies, and with most of the current standards [12–14,37]. Hence, the self-fabricated steel reinforcement and the locally available backfill soil could be used as the reinforced material for the MSE walls applied in the conditions of Vietnam.

Preprints (www.preprints.org) | NOT PEER-REVIEWED | Posted: 28 December 2023 doi:10.20944/preprints202312.2208.v1

Table 5. The length of reinforcement bars in the failure zone and backfill zone.

Depth (m)	Reinforcement layer	Full-scale model results		Current standards TCVN [14], AFNOR [12]	
		L_a (cm)	L_e (cm)	L_a (cm)	L_e (cm)
0.375	4	95	115	90	120
1.125	3	95	115	90	120
1.875	2	60	150	67.5	142.5
2.625	1	60	150	22.5	187.5

The correlation equation between the maximum tensile force in the reinforcement bars (F) and the depth (z) measured from the top of the wall is illustrated in Figure 11 and is shown in Eq. (5). The parabolic shape of the failure surface in the reinforced soil in this study is similar to the report of Murray and Farrar [7], and Chau, et al. [35].

$$z = 0.001F^2 - 0.3992F + 12.19 \quad (5)$$

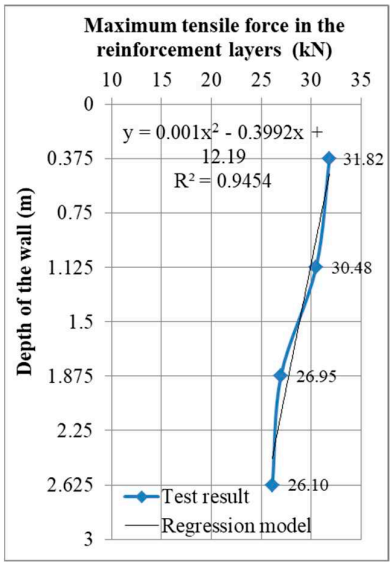

Figure 11. The trend line of the failure surface in the reinforced soil.

Lateral displacement of the wall facing

The experimental results indicate that the lateral displacement of the wall at the top of panel 2 (z = 1.5 m) is smaller than that at the top of panel 3 (z = 0.75 m), and the largest lateral displacement was observed at the top of panel 4 (top of the wall, z = 0 m) (as shown in Figure 12). At the failure load level (302 kN/m²), the maximum lateral displacement at the top of the wall was 3,899 μm, which is much smaller than the allowable lateral displacement for the wall (Δ = H/100 = 3 cm) [8,10]. The lateral displacement of the wall in this study has a similar pattern to the displacement profiles in the previous studies [36].

Preprints (www.preprints.org) | NOT PEER-REVIEWED | Posted: 28 December 2023 doi:10.20944/preprints202312.2208.v1

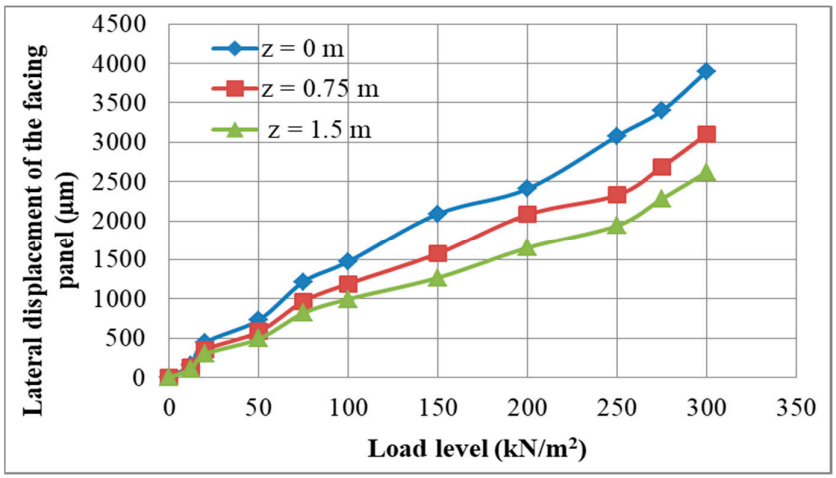

Figure 12. Lateral displacement of the wall facing.

4.2. Numerical model results

Figure 13 illustrates the lateral displacement of the wall facing and the tensile load distribution within the reinforcement layers during the construction of the wall (load level of 12 kN/m²). The numerical model results are similar to the report of Stuedlein, et al. [38].

Besides, at the maximum load level of 300 kN/m², the model results show that the highest lateral displacement of the wall facing was 4,270 mm as shown in Figure 14. In addition, the maximum tensile load in the forth reinforcement layer (near the top of the wall) was similar to the full-scale model and located at approximately 0.95m further away from the facing panel. This value decreases and closes to the wall facing the lower reinforcement layers as shown in Figure 10.

Figure 15 demonstrates that the simulation results are in good agreement with the measurement from the full-scale model. Thus, the findings from the study are reliable and could be used in practice. It indicates that the local backfill material and self-fabricated steel reinforcement could be used widely in the Central Region of Vietnam.

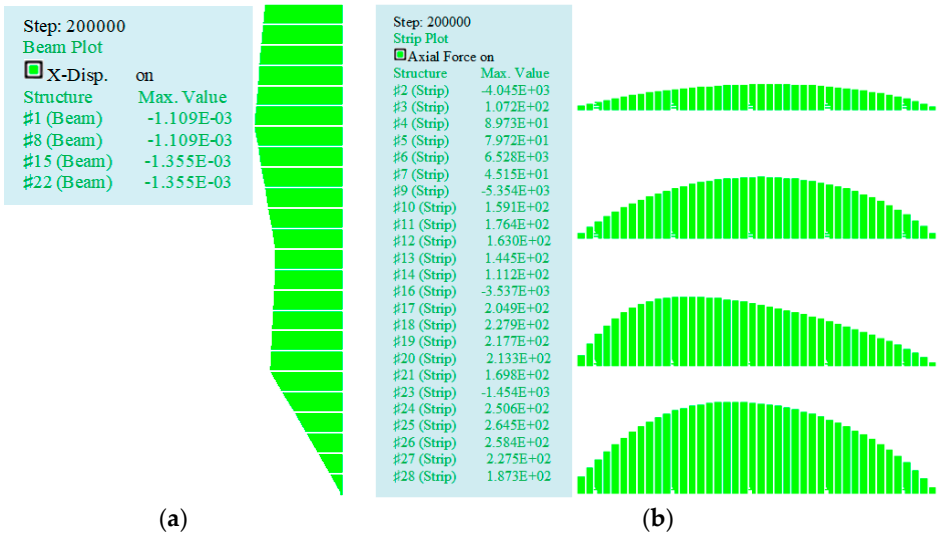

(**a**) (**b**)

Figure 13. The numerical model results during the construction of the wall. a. Displacement of the wall facing; b. Distribution of tensile force in the reinforcement layers.

Preprints (www.preprints.org) | NOT PEER-REVIEWED | Posted: 28 December 2023 doi:10.20944/preprints202312.2208.v1

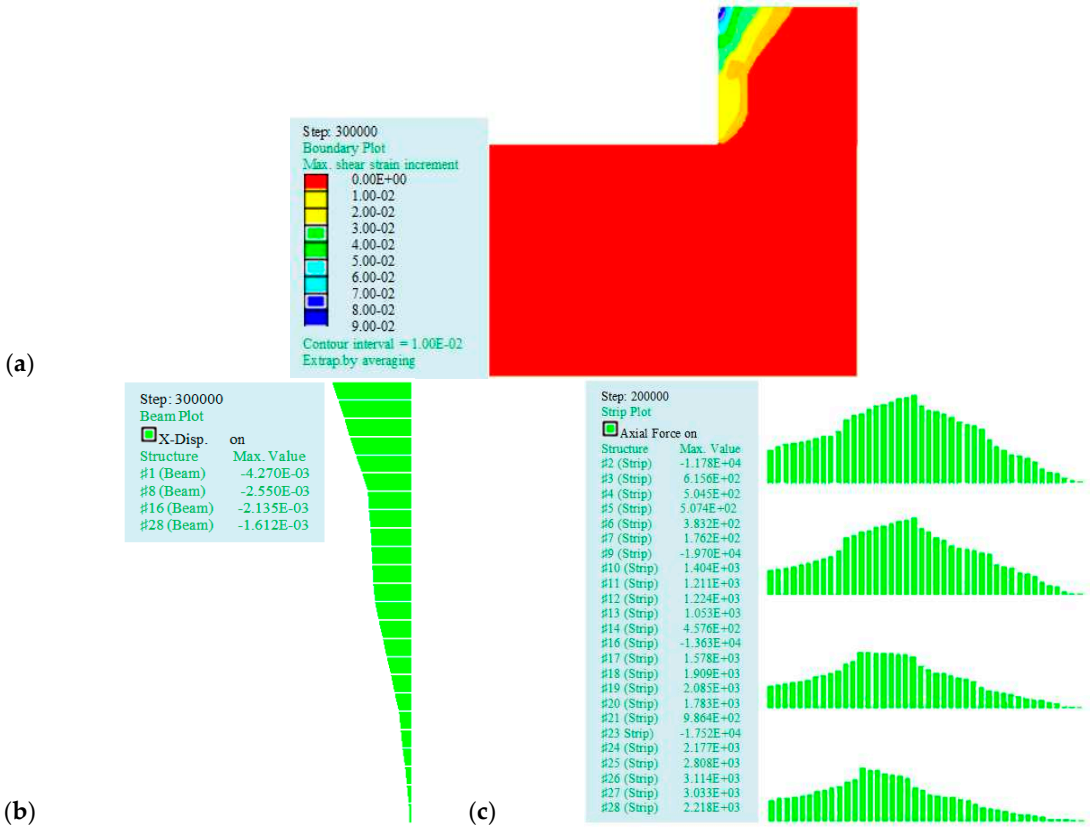

Figure 14. The numerical model results at the load level of 300 kN/m^2. a. Stress distribution in the retaining wall; b. Displacement of the wall facing; c. The distribution of the tensile force in the reinforcement layers.

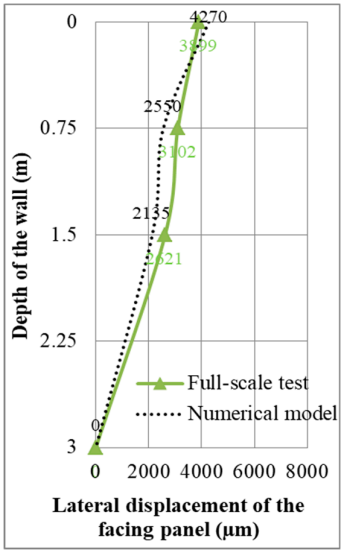

Figure 15. Lateral displacement of the wall facing from the physical and numerical models.

5. Conclusions

The paper presents the research results using a full-scale model and numerical model for the Mechanically Stabilized Earth (MSE) retaining wall with a self-fabricated galvanized steel reinforcement grid applied to low-cohesion soil in the Danang area.

 doi:10.20944/preprints202312.2208.v1

The experimental results show that the retaining wall suddenly collapsed due to internal instability (reinforcement rupture) at the load level of 302 kN/m², which is 15 times the design load. At that failure mode, the maximum lateral displacement at the top of the wall facing was 3,899 μm, which is much less than the allowable displacement of the wall (3 cm). The failure surface within the reinforced soil block is similar to theoretical studies.

In addition, the measured data from the full-scale model were validated by the numerical model by FLAC software. The tensile load distribution pattern in the reinforcement layer is similar to the research results from other studies and to be good in agreement with the current standards.

The experimental results also demonstrate that using the self-fabricated galvanized steel reinforcement (CB300V Φ10) for the MSE wall, considering the metal loss of 65% of the initial tensile strength, the wall still maintains its stability under the applied load. Deformations of the reinforcement are minimal, and the wall is capable of withstanding the high surcharge loads. Therefore, the self-fabricated galvanized steel reinforcement grids and the specific soil material in the Danang area could be used as the reinforcement material for the MSE wall with high stability.

Author Contributions: Conceptualization: Thu-Ha Nguyen; Data collection: Truong-Linh Chau and Thu-Ha Nguyen; Methodology: Thu-Ha Nguyen and Truong-Linh Chau; Supervision: Truong-Linh Chau; Writing – original draft: Van-Ngoc Pham; Writing – review & editing: Van-Ngoc Pham and Truong-Linh Chau.

Data Availability Statement: Some or all data, models, or codes that support the findings of this study are available from the corresponding author upon reasonable request.

Acknowledge: This work was supported by Ministry of Education and Training, The University of Danang, University of Science and Technology, the code number of Project: B2021-DNA-12.

Conflicts of Interest: The authors declare no conflict of interest.

Notations

The following symbols are used in this paper:
MSE walls = Mechanically Stabilized Earth Walls;
GSG = galvanized steel grid;
F_0= initial tensile strength of the reinforcement;
ΔF = proportional loss of tensile strength of the reinforcement;
L_a = the length of the reinforcement bars in the failure zone;
L_e = the length of the reinforcement bars in the backfill zone;
f* = the apparent friction coefficients for the steel reinforcement and backfill interfaces;
C_u = the coefficient of uniformity of the backfill soil;

Reference

1. Berg, R., Christopher, B., Samtani, N. "Design of Mechanically Stabilized Earth Walls and Reinforced Soil Slopes. ." edited by Volume II: Federal Highway Administration (FHWA), Washington, DC, 2009.
2. Chang, J. C., Forsyth, R., Smith, T. "Reinforced Earth Highway Embankment-Road 39." *Highway Focus* 4, no. 1 (1972): 15-35.
3. Chau, T.-L., Nguyen, T.-H., Vu, D.-P. "A Study on the Main Factors Affecting the Reinforcement Corrosion in Mechanically Stabilised Earth Walls and Predict the Service Life of the Wall." Paper presented at the CIGOS 2021, Emerging Technologies and Applications for Green Infrastructure: Proceedings of the 6th International Conference on Geotechnics, Civil Engineering and Structures. 2022.
4. Khan, B. J., Ahmad, M., Sabri, M. M. S., Ahmad, I., Zamin, B., Niekurzak, M. "Experimental and Numerical Evaluation of Mechanically Stabilized Earth Wall with Deformed Steel Bars Embedded in Tire Shred-Sand Mixture." *Buildings* 12, no. 5 (2022): 548. doi: https://doi.org/10.3390/buildings12050548.
5. Ahmadi, H., Bezuijen, A. "Full-Scale Mechanically Stabilized Earth (Mse) Walls under Strip Footing Load." *Geotextiles and Geomembranes* 46, no. 3 (2018): 297-311. doi: https://doi.org/10.1016/j.geotexmem.2017.12.002.
6. Mandloi, P., Sarkar, S., Hegde, A. "Performance Assessment of Mechanically Stabilised Earth Walls with Sustainable Backfills." *Proceedings of the Institution of Civil Engineers-Engineering Sustainability* 175, no. 6 (2022): 302-18. doi: https://doi.org/10.1680/jensu.22.00012.
7. Murray, R., Farrar, D. "Temperature Distributions in Reinforced Soil Retaining Walls." *Geotextiles and Geomembranes* 7, no. 1-2 (1988): 33-50. doi: https://doi.org/10.1016/0266-1144(88)90017-9.

8. Lee, K. L., Adams, B. D., Vagneron, J.-M. J. "Reinforced Earth Retaining Walls." *Journal of the Soil Mechanics and Foundations Division* 99, no. 10 (1973): 745-64.
9. Richards, D., Clayton, C., Powrie, W., Hayward, T. "Geotechnical Analysis of a Retaining Wall in Weak Rock." *Proceedings of the Institution of Civil Engineers-Geotechnical Engineering* 157, no. 1 (2004): 13-26. doi: https://doi.org/10.1680/geng.2004.157.1.13.
10. Ahmadi, H., Bezuijen, A., Zornberg, J. G. "Interaction Mechanisms in Small-Scale Model Mse Walls under the Strip Footing Load." *Geosynthetics International* 28, no. 3 (2021): 238-58. doi: https://doi.org/10.1680/jgein.20.00040.
11. Murray, R. "The Development of Specifications for Soil Nailing." In *TRL RESEARCH REPORT*, 1993.
12. AFNOR. "Geotechnical Design - Retaining Structures - Reinforced and Soil Nailing Structures." AFNOR NF P94-270:2020 (2020).
13. BSI. "Code of Practice for Strengthened/Reinforced Soils and Other Fills." BS 8006-1: 2010 (2010).
14. TCVN. "Highway Bridge Design Specification - Part 11: Abutments, Piers and Walls." TCVN 11823-11:2017 (2017).
15. Kibria, G., Hossain, M. S., Khan, M. S. "Influence of Soil Reinforcement on Horizontal Displacement of Mse Wall." *International Journal of Geomechanics* 14, no. 1 (2014): 130-41. doi: https://doi.org/10.1061/(ASCE)GM.1943-5622.0000297.
16. Roscoe, H., Twine, D. "Design and Performance of Retaining Walls." *Proceedings of the Institution of Civil Engineers-Geotechnical Engineering* 163, no. 5 (2010): 279-90. doi: https://doi.org/10.1680/geng.2010.163.5.279.
17. Jensen, J. A. Analysis of Full-Scale Mechanically Stabilized Earth (Mse) Wall Using Crimped Steel Wire Reinforcement: Utah State University, 2015.
18. Weldu, M. T. Pullout Resistance of Mse Wall Steel Strip Reinforcement in Uniform Aggregate. University of Kansas, 2015.
19. Ho, S., Rowe, R. K. "Effect of Wall Geometry on the Behaviour of Reinforced Soil Walls." *Geotextiles and Geomembranes* 14, no. 10 (1996): 521-41. doi: https://doi.org/10.1016/S0266-1144(97)83183-4.
20. Yu, Y., Bathurst, R. J., Miyata, Y. "Numerical Analysis of a Mechanically Stabilized Earth Wall Reinforced with Steel Strips." *Soils and Foundations* 55, no. 3 (2015): 536-47. doi: https://doi.org/10.1016/j.sandf.2015.04.006.
21. Weerasekara, L. "Improvements to Pullout Failure Estimation in Mse Walls." Paper presented at the The 71st Canadian Geotechnical Conference, Edmonton, BC. 2018.
22. Sadat, M. R., Huang, J., Bin-Shafique, S., Rezaeimalek, S. "Study of the Behavior of Mechanically Stabilized Earth (Mse) Walls Subjected to Differential Settlements." *Geotextiles and Geomembranes* 46, no. 1 (2018): 77-90. doi: https://doi.org/10.1016/j.geotexmem.2017.10.006.
23. Powrie, W., Chandler, R., Carder, D., Watson, G. "Back-Analysis of an Embedded Retaining Wall with a Stabilizing Base Slab." *Proceedings of the Institution of Civil Engineers-Geotechnical Engineering* 137, no. 2 (1999): 75-86. doi: https://doi.org/10.1680/gt.1999.370202.
24. Zhang, X., Chen, J., Liu, J. "Failure Mechanism of Two-Stage Mechanically Stabilized Earth Walls on Soft Ground." Paper presented at the Proceedings of the 8th International Congress on Environmental Geotechnics Volume 2. ICEG 2018 2019.
25. Tecco-5. "Effect of Reinforcement Types on the Mse Wall." In *Research report*: Transportation and Transport Infrastructure Design Consultancy Company, 2020.
26. AASHTO. "Standard Specification for Classification of Soils and Soil-Aggregate Mixtures for Highway Construction Purposes." *American Association of State and Highway Transportation Officials* M145-91 (2012).
27. Nguyen, T.-H., Chau, T.-L., Hoang, T., Nguyen, T. "Developing Artificial Neural Network Models to Predict Corrosion of Reinforcement in Mechanically Stabilized Earth Walls." *Neural Computing and Applications* 35, no. 9 (2023): 6787-99. doi: https://doi.org/10.1007/s00521-022-08043-1.
28. Chau, T.-L., Nguyen, T.-H. "Study the Influence of Adherence Edge to Steel Strip and Soil Interaction in Mechanically Stabilized Earth Wall with a Self-Made Strip." Paper presented at the CIGOS 2019, Innovation for Sustainable Infrastructure: Proceedings of the 5th International Conference on Geotechnics, Civil Engineering Works and Structures. 2020.
29. Haiun, G., Heurtebis, C., Renault, J. Les Ouvrages En Terre Armee-Guide Pour La Surveillance Specialisee Et Le Renforcement, 1994.
30. Itasca. "Flac-Fast Lagrangian Analysis of Continua, Version. 7.0." *Itasca Consulting Group Inc., Minneapolis* (2011).
31. Huang, B., Bathurst, R. J., Hatami, K. "Numerical Study of Reinforced Soil Segmental Walls Using Three Different Constitutive Soil Models." *Journal of geotechnical and geoenvironmental engineering* 135, no. 10 (2009): 1486-98. doi: https://doi.org/10.1061/(ASCE)GT.1943-5606.0000092.
32. Huang, B., Bathurst, R. J., Hatami, K., Allen, T. M. "Influence of Toe Restraint on Reinforced Soil Segmental Walls." *Canadian Geotechnical Journal* 47, no. 8 (2010): 885-904. doi: https://doi.org/10.1139/T10-002.
33. Schlosser, F. "La Terre Armee." *NOTE D'INF TECH* (1973).

34. Wichter, L., Risseuw, P., Guy, G. "Grossversuch Zurn Tragverhalten Einer Steilwand Aus Gewebe Und Mergel." Paper presented at the Proceedings of the Third International Conference on Geotextiles, Vienna, Austria 1986.
35. Chau, T., Corfdir, A., Bourgeois, E. "Corrosion Des Armatures Sur Le Comportement Des Murs En Terre Armée-Effect of Reinforcement Corrosion on the Behavior of Earth Walls Reinforced by Steel Elements (Soustitre: Scénarios De Corrosion Des Armatures Métalliques Et Les Dégradations Du Mur En Terre Armée)." *Éditions Universitaires Européennes (EUE)* (2016).
36. Schlosser, F., Guilloux, A. "Le Frottement Dans Le Renforcement Des Sols." *Revue française de Géotechnique*, no. 16 (1981): 65-77.
37. Naresh, C. S., Edward, A. N. "Mechanically Stabilized Earth (Mse) Wall Fills - a Framework for Use of Local Available Sustainable Resources (Lasr)." Washington, DC: Federal Highway Administration (FHWA), 2021.
38. Stuedlein, A. W., Bailey, M., Lindquist, D., Sankey, J., Neely, W. J. "Design and Performance of a 46-M-High Mse Wall." *Journal of geotechnical and geoenvironmental engineering* 136, no. 6 (2010): 786-96. doi: https://doi.org/10.1061/(ASCE)GT.1943-5606.0000294.